Amino Acid Residues 4425–4621 Localized on the Three-Dimensional Structure of the Skeletal Muscle Ryanodine Receptor

Brenda L. Benacquista,*† Manjuli R. Sharma,* Montserrat Samsó,* Francesco Zorzato,‡ Susan Treves,‡ and Terence Wagenknecht*†

*Wadsworth Center for Laboratories and Research, New York State Department of Health, Albany, New York 12201-0509 USA; †School of Public Health State University of New York at Albany, Albany, New York 12201-0509 USA; and ‡Institute of General Pathology, University of Ferrara, 44100 Ferrara, Italy

ABSTRACT We have localized a region contained within the sequence of amino acid residues 4425–4621 on the three-dimensional structure of the skeletal muscle ryanodine receptor (RyR). Mouse monoclonal antibodies raised against a peptide comprising these residues have been complexed with ryanodine receptors and imaged in the frozen-hydrated state by cryoelectron microscopy. These images, along with images of antibody-free ryanodine receptor, were used to compute two-dimensional averaged images and three-dimensional reconstructions. Two-dimensional averages of immunocomplexes in which the ryanodine receptor was in the fourfold symmetrical orientation disclosed four symmetrical regions of density located on the edges of the receptor's cytoplasmic assembly that were absent from control averages of receptor without added antibody. Three-dimensional reconstructions revealed the antibody-binding sites to be on the so-called handle domains of the ryanodine receptor's cytoplasmic assembly, near their junction with the transmembrane assembly. This study is the first to demonstrate epitope mapping on the three-dimensional structure of the ryanodine receptor.

INTRODUCTION

Ryanodine receptors (RyRs) are the major calcium release channels in striated muscle (for reviews see Fleischer and Inui, 1989; Meissner, 1994; Ogawa, 1994; Coronado et al., 1994; Franzini-Armstrong and Protasi, 1997; Wagenknecht and Radermacher, 1997; Shoshan-Barmatz and Ashley, 1998). They are the largest ion channels known, having net molecular masses of 2.3 MDa. The purified, detergent-solubilized skeletal receptor is composed of four identical copies of a large subunit (M_r 565 kDa) that are responsible for ion conduction and most of the receptor's pharmacological properties. Up to four copies of a small modulatory protein, identified as FKBP12, a 12-kDa FK506-binding protein, bind with nanomolar affinity to the receptor and copurify with it (Jayaraman et al., 1992). RyRs receive a signal upon depolarization of the transverse tubule that stimulates them to release calcium from the lumen of the sarcoplasmic reticulum (SR) into the myoplasm. The Ca^{2+} binds to the myofibrils, resulting in contraction of the muscle. Ligands such as Ca^{2+}, Mg^{2+}, ATP, calmodulin, and FKBP12 are known to bind to the isolated RyR and to modulate its activity (Liu et al., 1989; Smith et al., 1988; Jayaraman et al., 1992; Timerman et al., 1993; Tripathy et al., 1995).

Several laboratories, including our own, have determined three-dimensional reconstructions of RyR from skeletal muscle (RyR) to ~3-nm resolution from electron micrographs of negatively stained or frozen-hydrated, detergent-solubilized receptors (Wagenknecht et al., 1989, 1997; Radermacher et al., 1994; Wagenknecht and Radermacher, 1995; Serysheva et al., 1995; Orlova et al., 1996; Samsó and Wagenknecht, 1998). Unfortunately, correlation of the three-dimensional architecture of RyR with the sequence of its major subunit has been limited. To begin addressing this problem, we describe here the first reconstruction of RyR complexed with sequence-specific antibodies.

A region of the RyR sequence, residues 4425–4621, has been implicated in the calcium-dependent regulation of ion channel activity by directly binding Ca^{2+} and through interaction with Ca^{2+}-calmodulin (Zorzato et al., 1989; Fill et al., 1991; Treves et al., 1993; Menegazzi et al., 1994; Chen et al., 1992, 1993). These regulatory sites lie in the amino-terminal half of the fusion peptide, and in the native receptors are likely located in its cytoplasmic domains. The sequence 4425–4621 is also thought to contain one of the RyR's transmembrane segments, residues 4554–4575.

Here we have applied cyromicroscopy and image reconstruction techniques to immunocomplexes of RyR and a monoclonal antibody specific for residues 4425–4621 to map the location of this region of the RyR sequence on the three-dimensional architecture of the receptor. We find that there are four symmetrically positioned binding sites for the antibody located on the edges of the cytoplasmic assembly of the receptor, near its junction with the transmembrane region.

Received for publication 19 August 1999 and in final form 29 November 1999.

Address reprint requests to Brenda Benacquista, Wadsworth Center for Laboratories and Research, New York State Department of Health, Albany, NY 12201-0509. Tel.: 518-474-7895; Fax: 518-474-7992; E-mail: famolaro@wadsworth.org.

0006-3495/00/03/1349/10 $2.00

MATERIALS AND METHODS

Materials

The antibodies, raised against a fusion peptide corresponding to residues 4425–4621 of RyR, were prepared as described previously (Larini et al.,

1995), after immunization of Balb/c mice with fusion protein PC15 (Treves et al., 1993). The subclass of the monoclonal antibody was determined to be IgG1 with a mouse monoclonal antibody isotyping kit (catalog no. ISO-1; Sigma Immunochemicals, St. Louis, MO). For cryoelectron microscopy the antibody was concentrated approximately ninefold by ultrafiltration (Centricon 30 device; Amicon) after dialysis into a buffer consisting of 20 mM Tris-HCl (pH 7.5), 0.5 M KCl, 0.5 μg/ml leupeptin, and 2 mM dithiothreitol.

3-((Cholamidopropyl)dimethylammonio)-1-propane sulfate (CHAPS) was obtained from Calbiochem (La Jolla, CA). [^{3}H]Ryanodine (61.0 Ci/mmol) was from New England Nuclear. All other reagents were obtained from Sigma.

Rabbit RyRs were isolated from terminal cisternae vesicles of the SR (Saito et al., 1984) after solubilization in the presence of 4% CHAPS (Inui et al., 1987). The solubilized receptor was purified as previously described (Wagenknecht et al., 1997; Lai et al., 1988).

Western blot of terminal cisternae and bacterial cell extracts and immunoblotting using mAbI-29

DNA manipulations were carried out according to standard protocols as described by Maniatis et al. (1989). To cover the entire RyR coding sequence, we constructed a panel of RyR fusion proteins as previously described (Treves et al., 1993; Zorzato et al., 1996).

Competitive ELISA assay

The procedure was adapted from Grunwald and Meissner (1995). Microtiter plate wells (Corning polystyrene) were coated with purified RyR by drying 0.3 μg of receptor (0.5 pmol RyR subunit) from deionized water followed by fixation with 10% methanol. The wells were rinsed three times with TBS-T (Tris-buffered saline, 0.05% Tween-20), blocked by incubation with 5% dry milk in TBS overnight at 4°C, and washed again three times with TBS-T. Antibody mAbI29 (monoclonal mouse antibody raised against a peptide corresponding to residues 4425–4621 of the ryanodine receptor) (at 0.5 or 1.0 μg/ml) was incubated overnight at 4°C with RyRs (at 0, 0.2, 1.0, 2.0, and 10 μg/ml) in buffer containing 22.5 mM Na-3-(*N*-morpholino)propanesulfonic acid (pH 7.4), 0.15 M NaCl, 0.06 mM dithiothreitol, 0.05% CHAPS, 2.5 μg/ml leupeptin, and 1% nonfat dry milk. To each RyR-coated well was added 0.1 ml of one of the RyR-antibody mixtures, followed by 2 h of incubation at room temperature. The wells were washed and the amount of plate-bound antibody was quantified by the addition of IgG-alkaline phosphatase-labeled secondary antibody followed by color development with *p*-nitrophenyl phosphate, as recommended by the manufacturer (Sigma).

Immunoprecipitation of solubilized RyR by mAbI29 detected by radioassay

Purified RyR (0.45 μg) was incubated for 1 h at 23°C with mAbI29 included at 0.5, 1.0, 2.0, and 4.0-fold molar excess over RyR subunits in 65 μl of calcium-buffer F (final concentration: 20 mM Tris-Cl (pH 7.4), 0.5 M KCl, 2 mM dithiothreitol, 1 μg/ml leupeptin, 100 μM $CaCl_2$, and 1% (v/v) of [^{3}H]ryanodine at 12 nM (8.62 μCi/ml)). In the control reaction, rabbit IgG was substituted for mAbI29. Used as a secondary antibody, rabbit anti-mouse IgG at a concentration of 45 μg/ml was incubated with the immune complexes for 30 min at 4°C. Immune complexes were precipitated using 40 μl of a 50% (v/v) slurry of protein A-agarose (equilibrated versus calcium buffer F less ryanodine) incubated at 4°C for 1 h with agitation. The reaction supernatant was recovered, subjected to PEG precipitation (Shoshan-Barmatz and Zarka, 1992), and filtered through Whatman GF/B filters for detection of nonprecipitated protein-bound radioactivity. Each agarose pellet was washed three times with 400 μl of calcium buffer F less ryanodine. Recovered pellets were shaken in 10 ml of liquid scintillation cocktail and counted with a Beckman LS 9000 counter. Radioactivity of wash supernatants (100 μl) was also monitored.

Cryoelectron microscopy and image processing

Immunocomplexes were prepared by diluting RyRs 10-fold into concentrated mAbI29 such that the final protein concentrations were 0.05 mg/ml for RyR and 0.675 mg/ml for mAbI29 (molar ratio $\approx$ 50:1). The final buffer concentrations were 0.5 μg/ml leupeptin and 0.05% CHAPS. Control RyR was prepared identically, except that antibody was omitted. The reaction was incubated at room temperature for 15 min, and then 5-μl aliquots were applied to carbon-coated electron microscope grids and frozen (Radermacher et al., 1992, 1994). The grids were transferred to a Gatan model 626 cryoholder and analyzed by electron microscopy, using a Philips EM420 transmission electron microscope operated at 100 kV and a magnification of 52,000$\times$ (Wagenknecht et al., 1994). Untilted cryogrids were used to collect images for two-dimensional averaging of receptors in the fourfold symmetrical orientation, the most frequently occurring view. Images used for three-dimensional reconstructions were obtained from untilted cryogrids and from grids tilted by 30° in the microscope so as to increase the sampling of orientations.

Using the SPIDER software package (Frank, 1996), image processing was done as previously described (Wagenknecht et al., 1994; Sharma et al., 1998).

Two-dimensional averaged images of RyR and RyR:mAbI29 were computed using a homogenous data set of aligned fourfold symmetrical RyR images that had been classified by multivariate statistical analysis as previously described (Radermacher et al., 1994). The averaged RyR image was subtracted from that of RyR:mAbI29. Differences were considered statistically significant if they exceeded the standard error of the mean by a factor of 3, which corresponds to a significance level greater than 98% (Frank, 1996).

Three-dimensional reconstructions were determined using a projection matching technique (Penczek et al., 1994). In this technique a preexisting, three-dimensionally reconstructed RyR (Radermacher et al., 1994) was projected in a series of evenly spaced orientations. The RyR-mAbI29 images were individually matched to one of these projections and assigned the corresponding Eulerian angles for that projection. A three-dimensional reconstruction was then generated using these assigned angles. This procedure was iterated five times, using the reconstruction from the previous iteration to minimize the bias from the preexisting reconstruction used. The RyRs (without antibody) were processed independently by the same procedure to generate the control three-dimensional reconstruction. The resolution for three-dimensional (3D) reconstructions was determined using Fourier shell correlation with a cutoff value of 0.5 (Bottcher et al., 1997). Differences between reconstructions containing bound antibody and control reconstructions lacking antibody were analyzed in the same manner as other, previously characterized RyR-ligand complexes (Wagenknecht et al., 1997; Samsó et al., 1999).

RESULTS AND DISCUSSION

Characterization of mAbI29 specificity

We produced a monoclonal antibody against a fusion protein covering a region encompassed by residues 4425–4621, which have been demonstrated previously to be involved in the regulation of the RyR (Treves et al., 1993; Menegazzi et al., 1994). Lane 1 of Fig. 1 *B* shows that mAbI29 reacts strongly with the RyR present in the terminal cisternae fraction. To demonstrate that mAbI29 reacts with the epitope contained in the polypeptide defined by residues

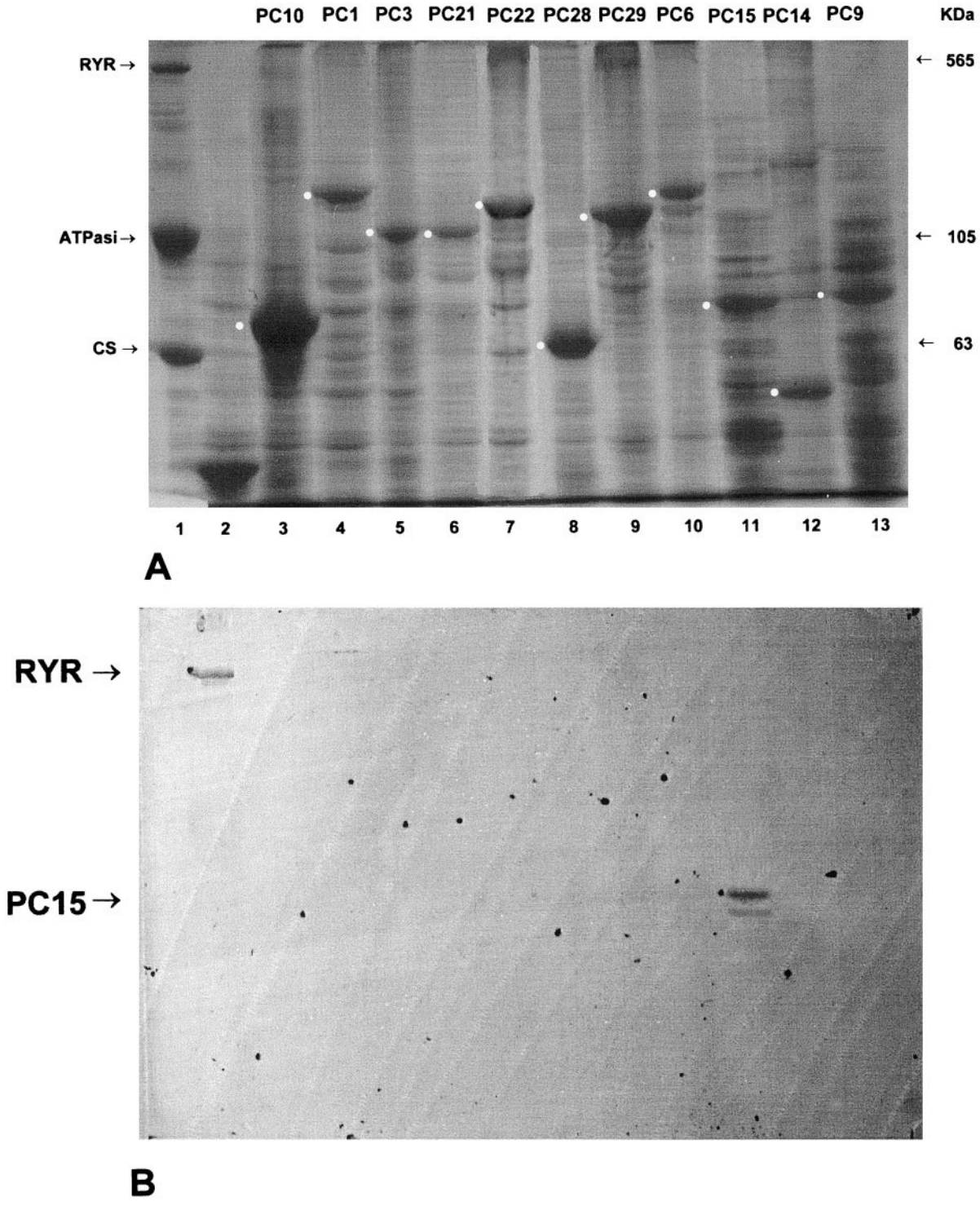

FIGURE 1 Western blot of terminal cisternae and bacterial cell extracts and immunoblotting characterization of mAbI29. The top line indicates the full-length rabbit RyR cDNA, and the segments below indicate the sizes of the RyR cDNA fragments cloned into the pATH bacterial expression vector (Menegazzi et al., 1994). Proteins in rabbit skeletal muscle terminal cisternae and bacterial cell extracts were electrophoretically separated by polyacrylamide gel electrophoresis in the presence of sodium dodecyl sulfate, transferred onto nitrocellulose filters, and reversibly stained with (*A*) Ponceau red and (*B*) indirect immunoenzymatic staining with mAbI29 (final concentration 1 μg/ml). *Lane 1*: 20 μg terminal cisternae; 20–50 μl of *E. coli* JM101 extracts were loaded on the gel. *Lane 2*: Extract from induced *E. coli* culture transfected with the pATH vector only. *Lanes 3–13*: *E. coli* extracts from induced culture with pATH RyR constructs; white dots indicate the fusion proteins in the extracts. *Lane 3*: PC10; *lane 4*: PC1; *lane 5*: PC3; *lane 6*: PC21; *lane 7*: PC22; *lane 8*: PC28; *lane 9*: PC29; *lane 10*: PC6; *lane 11*: PC15; *lane 12*: PC14; *lane 13*: PC9.

4425–4621, we probed it against a panel of fusion proteins covering the entire coding sequence of the RyR (Fig. 1 *A*). As expected, mAbI29 reacted only with its antigen (fusion protein PC15; Fig. 1 *B, lane 11*). mAbI29 did not recognize either the trpe bacterial protein (Fig. 1 *B, lane 2*), which was common to all of the fusion proteins, or any of the other RyR fusion proteins.

Before attempting to prepare immunocomplexes for cryomicroscopy, we tested the murine antibody mAbI29 for binding to the purified, detergent-solubilized RyR. A competitive enzyme-linked immunosorbent assay (ELISA) was performed in which mixtures of mAbI29 and solubilized RyR were incubated and then added to microtiter plate wells containing immobilized RyR. The amount of antibody bound to immobilized RyR was quantified by a colorimetric assay employing alkaline phosphatase-labeled secondary antibody (see Materials and Methods). The solubilized RyR was found to be an effective inhibitor of antibody binding to the immobilized receptor (Fig. 2 *A*).

To estimate the concentration of precipitating antibody, we performed immunoprecipitation experiments in which solubilized, [^{3}H]ryanodine-labeled RyR at the same concentration as would be used for cryoelectron microscopy was titrated with antibody. From the binding curve (Fig. 2 *B*), it was apparent that, at the highest antibody concentration, saturation of binding was not achieved. We concluded that it would be necessary to further concentrate the antibody to achieve the near-stoichiometric levels of binding that would be required for detection of RyR-bound antibody by cryoelectron microscopy. Ultrafiltration was used to concentrate the antibody solution approximately ninefold. Because of the limited amounts of antibody available, the concentrated material was used for microscopy without further characterization, except for gel electrophoresis to verify that the antibody was successfully concentrated (data not shown).

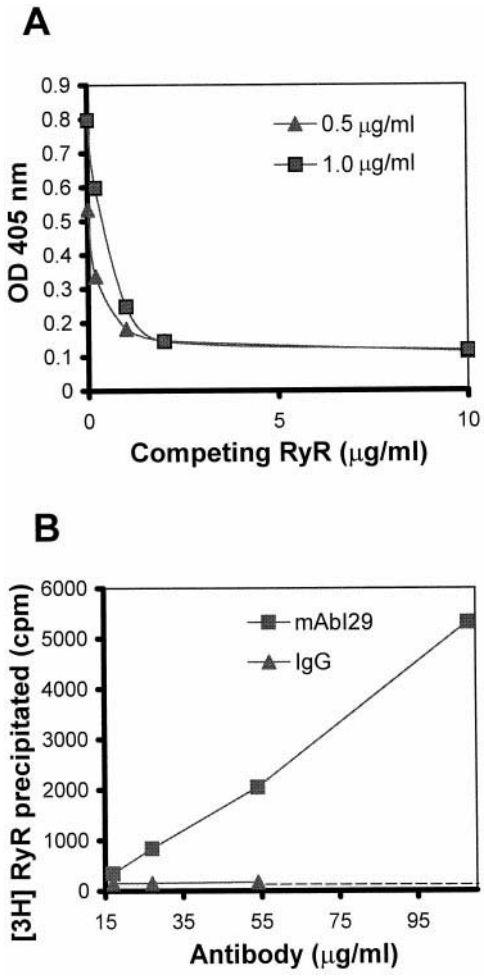

FIGURE 2 Characterization of antibody mAbI29 binding to RyR. (*A*) Competitive ELISA. RyRs were immobilized on microtiter plate wells and probed with mAbI29 (at concentrations of 0.5 and 1.0 μg/ml) containing solubilized RyR at the levels indicated on the abscissa. (*B*) A partial binding curve obtained by immunoprecipitation of [^{3}H]ryanodine-labeled RyR with increasing amounts of antibody mAbI29. Nonspecific rabbit IgG failed to precipitate significant amounts of RyR.

Cryoelectron microscopy and two-dimensional image analysis of RyR:mAbI29 complexes

Isolated RyR was incubated with and without (control) concentrated mAbI29, and aliquots of the reactions were applied to grids for cryo-EM (see Materials and Methods). For two-dimensional analysis, electron microscopy data were collected from nontilted specimen grids to maximize the number of fourfold symmetrical orientations. RyRs tend to adhere in orientations such that their fourfold symmetry axes are normal to the supporting carbon film. Fig. 3 *A* shows a selected area of an electron micrograph of isolated RyR, and Fig. 3 *B* shows a field of RyR:mAbI29 complexes (*arrows 1–3* indicate a few of the RyRs in fourfold orientations). The micrographs of RyR:mAbI29 differ from those of RyR alone in two ways. First, they contain substantial amounts of nonreceptor protein in the background, which is most likely due to the presence of protein that was not bound to the RyRs. Second, many of the RyRs appeared to be aggregated, probably as a result of interreceptor cross-linking by the antibodies. Efforts were made to isolate the ryanodine receptor-mAbI29 complex from the unbound antibodies by size exclusion chromatography and ultrafiltration, but electron microscopy showed that this treatment apparently damaged the RyRs. Despite the excess protein that was present in the RyR:mAbI29 mixture, a sufficient number of isolated, morphologically intact RyRs were easily identified in the micrographs.

Fig. 4, *A* and *B*, shows averages of fourfold symmetrized RyR:mAbI29 and RyR complexes, respectively. Fig. 4 *C* shows a difference map obtained after the averaged image of RyR was subtracted from that of RyR:mAbI29. Light (*white*) regions indicate mass present in the RyR-mAbI29

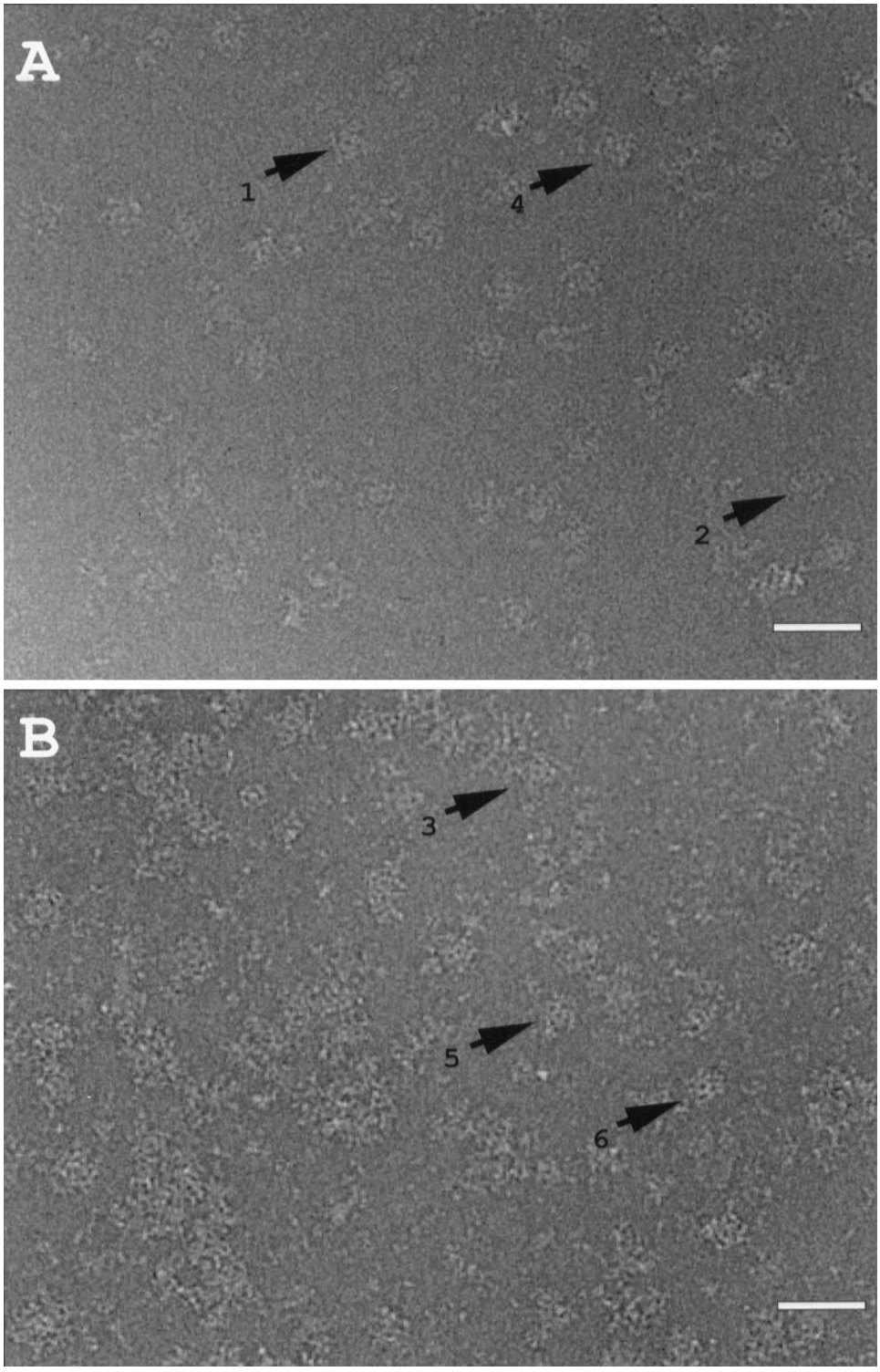

FIGURE 3 Cryoelectron microscopy of RyR and RyR:mAbI29: portions of micrographs of (*A*) isolated RyR and (*B*) RyR:mAbI29 complexes. Arrows 1, 2, and 3 mark ryanodine receptors in the fourfold symmetrical orientation used for two-dimensional averaging. Arrows 4, 5, and 6 denote ryanodine receptors in nonfourfold orientations, which are required for three-dimensional reconstruction. Scale bar, 700 Å.

complex that is absent from RyR. As seen in Fig. 4 *C*, four symmetrically disposed regions dominate the difference image. The density associated with these differences is more than twice that of any other positive differences. A statistical analysis (see Materials and Methods) of the difference image indicates that these four regions are significant with a confidence level greater than 98% (Fig. 4 *D*). We attribute these highly significant and localized regions of difference to the excess mass contributed by mAbI29 and consider them to be indicative of the location of an epitope contained within amino acid residues 4425–4621, to which the antibody was raised.

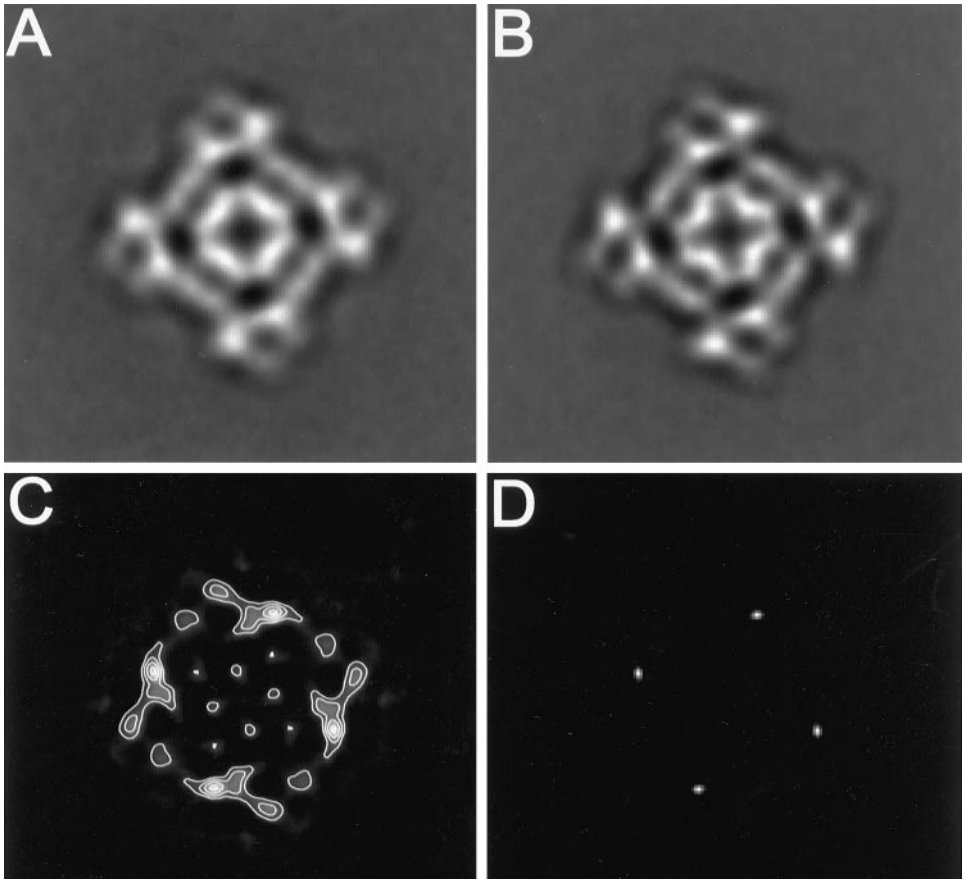

FIGURE 4 Two-dimensional image averaging of RyR:mAbI29 and RyR. (*A*) Average of RyR:mAbI29 complex ($N = 119$). (*B*) Average of RyR ($N = 234$). (*C*) Difference map with contours superimposed, formed by subtracting the two-dimensional reconstruction in *B* from that in *A*. Note that the four symmetrically disposed regions of highest difference are more than twice as large as any other differences. (*D*) The most significant statistical differences (>98% significance level) in *C*, determined as described in Materials and Methods (*white regions*). Scale bar, 150 Å.

Three-dimensional reconstruction of RyR:mAbI29 complexes

The image obtained by averaging RyR:mAbI29 complexes in the fourfold-symmetrical orientation does not define the location of the bound antibody in the direction parallel to the axis of symmetry (which we define as the *z* direction), and therefore, 3D reconstructions were determined for control and RyR:mAbI29 immunocomplexes. To obtain a sufficient number of non-fourfold-symmetrical views (e.g., Fig. 3, *arrows 4–6*), which are essential for 3D reconstruction, micrographs were recorded with the specimen grids tilted by 30°. The individual images were extracted from the micrographs and used to compute a 3D reconstruction (see Materials and Methods).

Representations of the 3D reconstructions obtained for RyR without added antibody and for RyR:mAbI29 are similar when displayed as solid bodies, and by examination it is not obvious where the mass contributed by bound antibody is located (Fig. 5, *A* and *B*). The reconstructions show that the RyR comprises two main components, a transmembrane region or assembly (labeled TA) and a larger cytoplasmic assembly containing at least 10 distinct domains (labeled 1–10), each present four times, as dictated by the quaternary structure of the receptor. These features are essentially identical to results of prior reconstructions from our laboratory (Radermacher et al., 1994; Wagenknecht et al., 1997). Reconstructions determined under these conditions resemble those of the "closed" state of the receptor described previously (Orlova et al., 1996) and confirmed in our own laboratory (Sharma and Wagenknecht, unpublished results). Several structural features appear slightly enlarged in the RyR:mAbI29 reconstruction relative to the RyR reconstruction—for example, the transmembrane assembly and domains 3, 6, and 10 in the cytoplasmic region. These differences in overall shape probably are not attributable to changes induced by binding of antibodies in a specific manner, but more likely arise from the large amount of excess protein that was present in the solution of antibody that was added to the receptor (Fig. 3), some of which might have interacted nonspecifically with the receptor. Subtraction of the two reconstructions was necessary to determine the areas of greatest, and presumably most significant, localized differences in density between the two reconstructions. Fig. 5 *C* shows the reconstruction of RyR without added antibody together with the largest differences attributed to bound mAbI29 superimposed (*purple regions*). The regions of greatest difference are associated with the domains labeled 3, also referred to as the "handles" (Orlova et al., 1996). When the 3D difference map is projected in the *z* direction, the differences associ-

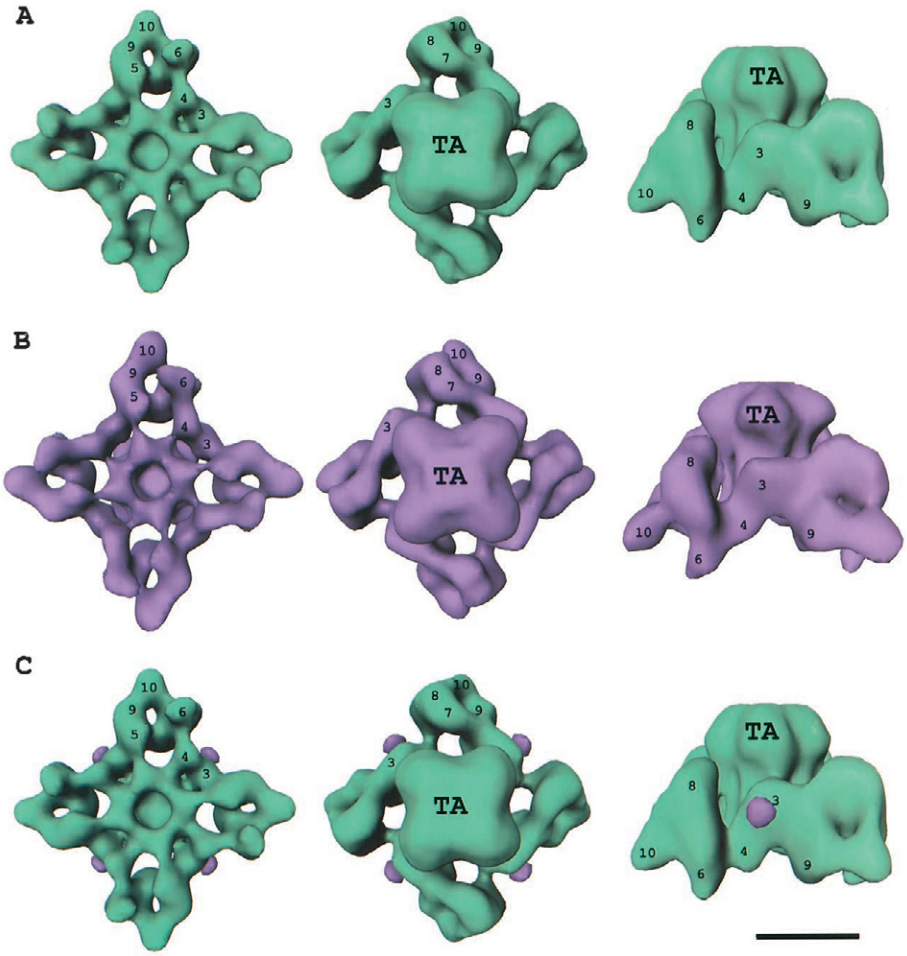

FIGURE 5 Three-dimensional reconstructions of RyR and RyR:mAbI29. (*A*) Three-dimensional reconstruction of isolated RyR ($N = 2852$), showing cytoplasmic-facing (*left*), sarcoplasmic reticulum-facing (*middle*), and side (*right*) views. (*B*) Three-dimensional reconstruction of RyR-mAbI29 ($N = 2065$), shown in the same orientations as in *A*. (*C*) As in *A*, except that the differences (obtained by subtracting the reconstruction in *A* from the reconstruction in *B*) are superimposed. Shown is the entire difference image obtained at the chosen threshold, which was selected to reveal the strongest differences. Scale bar, 150 Å.

ated with the handles lie at the same locations as the major differences that were observed in the two-dimensional averaged images. This agreement of the two- and three-dimensional analyses is further evidence that these regions of excess density are highly significant because there is little overlap between the two data sets. Thus the main density differences that are associated with the handles represent the most likely locations for the epitope that is recognized by mAbI29.

The density attributed to bound antibody in the reconstruction of RyR:mAbI29 is weaker and more diffuse than might be expected based solely upon the resolution of the reconstruction, estimated at 34 Å. It is not unusual in studies of this type for only the Fab portion of the antibody that is binding to the substrate to be clearly resolved. When the antibody binds to the RyR, the distal portion of the antibody is quite flexible and assumes many different positions, resulting in blurring. For the RyR:mAbI29 reconstruction even the proximal Fab arm has not been fully resolved. Other studies involving 3D reconstruction of immunocomplexes by electron microscopy have reported findings similar to those described here, whereas in others the Fab portion of the antibody has been resolved with sufficient clarity to allow fitting of atomic models of Fab fragments into the density envelope (for a recent discussion see Yu et al., 1998). One possible explanation for less than optimal visualization of mAbI29 in 3D reconstructions is that the antibody was bound to a mobile region of the RyR, and hence regions distal to its point of attachment were not as well resolved as proximal regions. Indeed, potential unstructured mobile segments, rich in the amino acids glycine, alanine, and proline, are found within the RyR amino acid sequence to which mAbI29 was raised (Treves et al., 1993). Moreover, this sequence lies within a region (residues 4254–4631, which has been termed divergency region 1) that varies more than any other among the three isoforms of the ryanodine receptor (Sorrentino and Volpe, 1993). Finally, it is possible that the low density contributed by bound antibody in the reconstructions was due to substoichiometric occupancy of its epitopes on RyR due to partial dissociation of antibodies that occurred upon adsorption to the specimen grid.

Taking the preceding considerations into account, we conclude that some portion of the sequence 4425–4621 is contained within domain 3 (handle domain) of the RyR, at a region that is proximal to the transmembrane assembly

(see below). The three-dimensional analysis was repeated with a different set of images to check experimental reproducibility, with essentially identical results.

Comparison of experimental results with previous studies

A location on domain 3 of the RyR for residues 4425–4621 seems reasonable when other information bearing on this region of the sequence is considered. First, there is compelling evidence that parts of this sequence are surface-exposed and on the cytoplasmic side of the SR. The epitope recognized by mAbI29 is readily accessible in vesicles derived from terminal cisternae of skeletal-muscle SR. Polyclonal antibodies raised to the peptide that was used to obtain mAbI29 were found to influence in vitro the activity of the channel in response to Ca^{2+}, implicating the sequence 4425–4621 in regulation of the RyR (Treves et al., 1993). In addition to accessibility by mAbI29, the sequence 4425–4621 contains sites at residues Lys^{4474} and Arg^{4475} that are readily cleaved when proteases are added to isolated RyR or RyR that is present in SR-derived vesicles (Marks et al., 1990).

Besides surface-exposed residues, the sequence 4425–4621 is thought to contain one of the transmembrane segments of the RyR; specifically, residues 4554–4575 are among the most hydrophobic stretches found in the entire RyR sequence, and experimental evidence that residues adjoining the carboxy side of this sequence are located in the lumen of the SR has been reported (Takeshima et al., 1989; Zorzato et al., 1990; Grunwald and Meissner, 1995).

The preceding discussion, when combined with our 3D localization of mAbI29 binding sites, suggests the following model for the topology of the sequence 4425–4621 in the RyR (Fig. 6). The antibody binding location found on domain 3 of the 3D reconstruction (Fig. 5) probably corresponds to the amino-terminal portion of the sequence 4425–4621 (*pink dot* in Fig. 6), upstream of residues 4554–4575, which form the putative transmembrane segment (*zigzag line* in Fig. 6). The carboxy-terminal 46 residues (4576–4621) are predicted to be located mostly in the lumen of the SR (*pink loop following the zigzag line* in Fig. 6), according to current models of the transmembrane topology of RyR (Zorzato et al., 1990; Takeshima et al., 1989; Grunwald and Meissner, 1995; Brandt et al., 1992). A bridge of density spanning the region between domain 3 and the transmembrane assembly appears to connect the two regions.

At least six potential calmodulin-binding sites, widely separated in the sequence of the RyR, have been proposed based upon experiments involving calmodulin binding to peptides derived from the RyR's amino acid sequence (Chen and MacLennan, 1994; Menegazzi et al., 1994; Guerrini et al., 1995). However, experimental support that calmodulin binds to any of these sequences in the native receptor is lacking, and even the number of distinct calmodulin-binding sites on the intact receptor is uncertain (Yang et al., 1994; Tripathy et al., 1995; Moore et al., 1999). The bacterially expressed fusion protein, corresponding to the RyR sequence 4425–4621, that was used as an antigen to obtain mAbI29, is one of the peptides that has been shown to bind calmodulin (Menegazzi it al., 1994). Thus it is possible that the mAbI29-binding site that we have determined in this study is at or near a calmodulin-binding site on the RyR. In a previous study from this laboratory (Wagenknecht et al., 1994, 1997), a RyR:calmodulin complex was characterized by 3D reconstruction, and the calmodulin was found to bind in the crevice formed between domain 3 and the "clamp" region that forms each of the corners of the cytoplasmic assembly (indicated by the *asterisk* in Fig. 6). This site is clearly distinct from the mAbI29-binding site found in this study. Based on our model for the location and topology of the sequence corresponding to RyR residues 4425–4461 (Fig. 6), it appears unlikely that this sequence could extend to the calmodulin site mapped previously. Thus, if the site defined by mAbI29 does indeed correspond to a calmodulin site, then it is a different site from the one detected in our earlier study.

Further cryo-immuno-electron microscopic studies employing antibodies specific for other surface-exposed regions of the RyR sequence should lead to a detailed model for which segments of the sequence form the various domains that comprise the receptor.

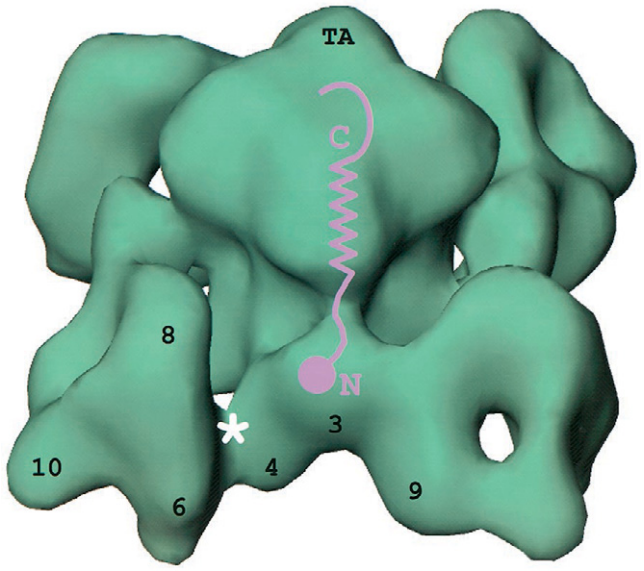

FIGURE 6 Model for topology of residues 4425–4621, superimposed on the 3D model of RyR. This schematic model indicates the three-dimensional location for sequence 4425–4621 of the skeletal muscle ryanodine receptor. The dot indicates the antibody-binding region, which is proposed to correspond to the amino-terminal region (indicated by N) of the sequence. C denotes the carboxy-terminal portion of the sequence. The asterisk indicates the CaM-binding site identified in previous studies (see text).

We thank Jon Berkowitz for technical support with the immunological characterization of the antibody.

These studies were supported by National Institutes of Health grant AR40615 (TW); Telethon-Italy project 617, Ministero dell'Universita e della Ricerca Scientifica e Tecnologica (MURST) (FZ); grant ERBFMRXCT960032 from the European Union (FZ); and the American Heart Association Fellowship #960124 (to M.R.S.). We thankfully acknowledge the use of the Wadsworth Center's Electron Microscopy, Research Computing, and Biochemistry core facilities.

REFERENCES

Bottcher, B., S. A. Wynne, and R. A. Crowther. 1997. Determination of the fold of the core protein of hepatitis B virus by electron cryomicroscopy. *Nature.* 386:88–91.

Brandt, N. R., A. H. Caswell, T. Brandt, K. Brew, and R. L. Mellgren. 1992. Mapping of the calpain proteolysis product of the junctional foot protein of the skeletal muscle triad junction. *J. Membr. Biol.* 127:35–47.

Chen, S. R., and D. H. MacLennan. 1994. Identification of calmodulin, Ca^{2+}- and ruthenium red-binding domains in the Ca^{2+} release channel (ryanodine receptor) of rabbit skeletal muscle sarcoplasmic reticulum. *J. Biol. Chem.* 269:22698–22704.

Chen, S. R., L. Zhang, and D. H. MacLennan. 1992. Characterization of a Ca^{2+} binding and regulatory site in the Ca^{2+} release channel (ryanodine receptor) of rabbit skeletal muscle sarcoplasmic reticulum. *J. Biol. Chem.* 267:23318–23326.

Chen, S. R., L. Zhang, and D. H. MacLennan. 1993. Antibodies as probes for Ca^{2+} activation sites in the Ca^{2+} release channel (ryanodine receptor) of rabbit skeletal muscle sarcoplasmic reticulum. *J. Biol. Chem.* 268:13414–13421.

Coronado, R., J. Morrissette, M. Sukhareva, and D. M. Vaughan. 1994. Structure and function of ryanodine receptors. *Am. J. Physiol.* 266: C1485–C1504.

Fill, M., R. Meja-Alvarez, F. Zorzato, P. Volpe, and E. Stefani. 1991. Antibodies as probes for ligand gating of single sarcoplasmic reticulum Ca^{2+}-release channels. *Biochem. J.* 273:449–457.

Fleischer, S., and M. Inui. 1989. Biochemistry and biophysics of excitation-contraction coupling. *Annu. Rev. Biophys. Biophys. Chem.* 18: 333–364.

Frank, J. 1996. Three-Dimensional Electron Microscopy of Macromolecular Assemblies. Academic Press, San Diego.

Franzini-Armstrong, C., and F. Protasi. 1997. Ryanodine receptor of striated muscles: a complex channel capable of multiple interactions. *Physiol. Rev.* 77:699–729.

Grunwald, R., and G. Meissner. 1995. Lumenal sites and C terminus accessibility of the skeletal muscle calcium release channel (ryanodine receptor). *J. Biol. Chem.* 270:11338–11347.

Guerrini, R., P. Menegazzi, R. Anacardio, M. Marastoni, R. Tomatis, F. Zorzato, and S. Treves. 1995. Calmodulin binding sites of the skeletal, cardiac, and brain ryanodine receptor Ca^{2+} channels: modulation by the catalytic subunit of cAMP-dependent protein kinase? *Biochemistry.* 34: 5120–5129.

Inui, M., A. Saito, and S. Fleischer. 1987. Purification of the ryanodine receptor and identity with feet structures of junctional terminal cisternae of sarcoplasmic reticulum from fast skeletal muscle. *J. Biol. Chem.* 262:1740–1747.

Jayaraman, T., A.-M. Brillantes, A. P. Timerman, S. Fleischer, H. Erdjument-Bromage, P. Tempst, and A. R. Marks. 1992. FK506 binding protein associated with the calcium release channel (ryanodine receptor). *J. Biol. Chem.* 267:9474–9477.

Lai, F. A., H. P. Erickson, E. Rousseau, Q. Y. Liu, and G. Meissner. 1988. Purification and reconstitution of the calcium release channel from skeletal muscle. *Nature.* 331:315–319.

Larini, F., P. Menegazzi, O. Baricordi, F. Zorzato, and S. Treves. 1995. A ryanodine receptor-like Ca^{2+} channel is expressed in nonexcitable cells. *Mol. Pharmacol.* 47:21–28.

Liu, Q. Y., F. A. Lai, E. Rousseau, R. V. Jones, and G. Meissner. 1989. Multiple conductance states of the purified calcium release channel complex from skeletal sarcoplasmic reticulum. *Biophys. J.* 55:415–424.

Maniatis, T., E. F. Fritsch, and J. Sambrook. 1989. Molecular Cloning: A Laboratory Manual, 2nd Ed. Cold Spring Harbor Laboratory, Cold Spring Harbor, NY.

Marks, A. R., S. Fleischer, and P. Tempst. 1990. Surface topography analysis of the ryanodine receptor/junctional channel complex based on proteolysis sensitivity mapping. *J. Biol. Chem.* 265:13143–13149.

Meissner, G. 1994. Ryanodine receptor Ca^{2+} release channels and their regulation by endogenous effectors. *Annu. Rev. Physiol.* 56:485–508.

Menegazzi, P., F. Larini, S. Treves, R. Guerrini, M. Quadroni, and F. Zorzato. 1994. Identification and characterization of three calmodulin binding sites of the skeletal muscle ryanodine receptor. *Biochemistry.* 33:9078–9084.

Moore, C. P., G. Rodney, J.-Z. Zhang, L. Santacruz-Toloza, G. Strasburg, and S. L. Hamilton. 1999. Apocalmodulin and Ca^{2+} calmodulin bind to the same region on the skeletal muscle Ca^{2+} release channel. *Biochemistry.* 38:8532–8537.

Ogawa, Y. 1994. Role of ryanodine receptors. *Crit. Rev. Biochem. Mol. Biol.* 29:229–274.

Orlova, E., I. Serysheva, M. Van Heel, S. Hamilton, and W. Chiu. 1996. Two structural configurations of the skeletal muscle calcium release channel. *Nature Struct. Biol.* 3:547–552.

Penczek, P. A., R. Grassucci, and J. Frank. 1994. The ribosome at improved resolution: new techniques for merging and orientation refinement in 3D cryo-electron microscopy of biological particles. *Ultramicroscopy.* 53:251–270.

Radermacher, M., V. Rao, R. Grassucci, J. Frank, A. P. Timerman, S. Fleischer, and T. Wagenknecht. 1994. Cryo-electron microscopy and three-dimensional reconstruction of the calcium release channel ryanodine receptor from skeletal muscle. *J. Cell Biol.* 127:411–423.

Radermacher, M., T. Wagenknecht, R. Grassucci, J. Frank, M. Inui, C. Chadwick, and S. Fleischer. 1992. Cryo-EM of the native structure of the calcium release channel/ryanodine receptor from the sarcoplasmic reticulum. *Biophys. J.* 61:936–940.

Saito, A., S. Seiler, A. Chu, and S. Fleischer. 1984. Preparation and morphology of sarcoplasmic reticulum terminal cisternae from rabbit skeletal muscle. *J. Cell Biol.* 99:975–985.

Samsó, M., R. Trujillo, G. B. Gurrola, H. H. Valdivia, and T. Wagenknecht. 1999. Three-dimensional location of the imperatoxin A binding site on the ryanodine receptor. *J. Cell Biol.* 146:493–500.

Samsó, M., and T. Wagenknecht. 1998. Contributions of electron microscopy and single-particle techniques to the determination of the ryanodine receptor three-dimensional structure. *J. Struct. Biol.* 121:172–180.

Serysheva, I. I., E. V. Orlova, W. Chiu, M. B. Sherman, S. L. Hamilton, and M. Van Heel. 1995. Electron cryomicroscopy and angular reconstitution used to visualize the skeletal muscle calcium release channel. *Struct. Biol.* 2:18–24.

Sharma, M., P. Penczek, R. Grassucci, H. B. Xin, S. Fleischer, and T. Wagenknecht. 1998. Cryoelectron microscopy and image analysis of the cardiac ryanodine receptor. *J. Biol. Chem.* 273:18429–18343.

Shoshan-Barmatz, V., and R. H. Ashley. 1998. The structure, function, and cellular regulation of ryanodine-sensitive Ca^{2+} release channels. *Int. Rev. Cytol.* 183:185–271.

Shoshan-Barmatz, V., and A. Zarka. 1992. A simple, fast, one-step method for the purification of the skeletal-muscle ryanodine receptor. *Biochem. J.* 285:61–64.

Smith, J. S., T. Imagawa, J. Ma, M. Fill, K. P. Campbell, and R. Coronado. 1988. Purified ryanodine receptor from rabbit skeletal muscle is the calcium-release channel of sarcoplasmic reticulum. *J. Gen. Physiol.* 92:1–26.

Sorrentino, V., and P. Volpe. 1993. Ryanodine receptors—how many, where and why? *Trends Pharmacol. Sci.* 14:98–103.

Takeshima, H., S. Nishimura, T. Matsumoto, H. Ishida, K. Kangawa, N. Minamino, H. Matsuo, M. Veda, M. Hanaoka, T. Hirose, and S. Numa. 1989. Primary structure and expression from complementary DNA of skeletal muscle ryanodine receptor. *Nature.* 339:439–445.

Timerman, A. P., E. Ogunbumni, E. Freund, G. Wiederrecht, A. R. Marks, and S. Fleischer. 1993. The calcium release channel of sarcoplasmic reticulum is modulated by FK-506-binding protein. Dissociation and reconstruction of FKBP-12 to the calcium release channel of skeletal muscle sarcoplasmic reticulum. *J. Biol. Chem.* 268:22992–22999.

Treves, S., P. Chiozza, and F. Zorzato. 1993. Identification of the domain recognized by anti- (ryanodine receptor) antibodies which affect Ca^{2+}-induced Ca^{2+} release. *Biochem. J.* 291:757–763.

Tripathy, A., L. Xu, G. Mann, and G. Meissner. 1995. Calmodulin activation and inhibition of skeletal muscle Ca^{2+} release channel (ryanodine receptor). *Biophys. J.* 69:106–119.

Wagenknecht, T., J. Berkowitz, R. Grassucci, A. P. Timerman, and S. Fleischer. 1994. Localization of calmodulin binding sites on the ryanodine receptor from skeletal muscle by electron microscopy. *Biophys. J.* 67:2286–2295.

Wagenknecht, T., R. Grassucci, J. Frank, A. Saito, M. Inui, and S. Fleischer. 1989. Three-dimensional architecture of the calcium channel/foot structure of the sarcoplasmic reticulum. *Nature.* 338:167–170.

Wagenknecht, T., and M. Radermacher. 1995. Three-dimensional architecture of the skeletal muscle ryanodine receptor. *FEBS Lett.* 369:43–46.

Wagenknecht, T., and M. Radermacher. 1997. Ryanodine receptors-structure and macromolecular interactions. *Curr. Opin. Struct. Biol.* 7:258–265.

Wagenknecht, T., M. Radermacher, R. Grassucci, J. Berkowitz, H. B. Xin, and S. Fleischer. 1997. Locations of calmodulin and FK506-binding protein on the three-dimensional architecture of the skeletal muscle ryanodine receptor. *J. Biol. Chem.* 272:32463–32471.

Yang, H.-C., M. M. Reedy, C. L. Burke, and G. M. Strasburg. 1994. Calmodulin interaction with the skeletal muscle sarcoplasmic reticulum calcium channel protein. *Biochemistry.* 33:518–525.

Yu, X., T. Shibata, and E. H. Egelman. 1998. Identification of a defined epitope on the surface of the active recA-DNA filament using a monoclonal antibody and three-dimensional reconstruction. *J. Mol. Biol.* 283:985–992.

Zorzato, F., A. Chu, and P. Volpe. 1989. Antibodies to junctional sarcoplasmic reticulum proteins: probes for the Ca^{2+}-release channel. *Biochem. J.* 261:863–870.

Zorzato, F., J. Fujii, K. Otsu, M. Phillips, N. M. Green, F. A. Lai, G. Meissner, and D. H. MacLennan. 1990. Molecular cloning of cDNA encoding human and rabbit forms of the Ca^{2+} release channel (ryanodine receptor) of skeletal muscle sarcoplasmic reticulum. *J. Biol. Chem.* 265:2244–2256.

Zorzato, F., P. Menegazzi, S. Treves, and M. Ronjat. 1996. Role of malignant hyperthermia domain in the regulation of Ca^{2+} release channel (ryanodine receptor) of skeletal muscle sarcoplasmic reticulum. *J. Biol. Chem.* 271:22759–22763.